ARTICLE

DOI: 10.1590/2317-488920202020190114

BJGEO Brazilian Journal of Geology

Potential development of green and purple colors in colorless natural quartz from geodes in rhyodacites, Serra Geral Group, Brazil

Larissa Lanes Tononi[1]*, Lauren da Cunha Duarte[1,2], Pedro Luiz Juchem[2], Fernando Soares Lameiras[3], Jurgen Schnellrath[4], Mauricio Thadeu Fenilli de Menezes[1]

Abstract

Colorless quartz can develop a green color when submitted to gamma irradiation and its development is related to the presence of molecular water and hydroxyl groups in the quartz crystalline structure. In the present study, colorless quartz crystals hosted in geodes within rhyodacites of Serra Geral Group, Southern Brazil, were selected to test the potential development of green color. The samples were analyzed by infrared (IR) and thermogravimetric (TGA) techniques, in addition to the Amethyst Factor (f_a) method. All samples showed an absorption bands in the IR, indicating possible development of a green or purple color, and f_a analysis indicated the samples would develop a green color. All samples became colored after irradiation, presenting color zoning: from colorless to grayish-green, and from grayish-green to slightly purplish. Some samples showed a greenish colored zone and developed an amethyst phantom crystal in its apical portion. In addition, a high content of water in samples that remained colorless after irradiation was detected. It is here interpreted that water concentration varied during quartz crystallization, enabling the development of the green color, and that the excess of water can inhibit the development of radiation-induced color in colorless natural quartz crystals.

KEYWORDS: Quartz; green quartz, amethyst, infrared spectroscopy; irradiation.

INTRODUCTION

Quartz can develop a variety of colors, one of those being a grayish-green color induced by gamma irradiation. The development of grayish-green color is related to the presence of hydroxyl groups (OH) or molecular water in the crystalline structure (Salh 2011, Enokihara 2013). According to Henn and Schultz-Güttler (2012), the molecular water is associated with substitutional and interstitial defects in channels of the quartz structure, twin planes, or micro-structural growth defects. In quartz crystals with high hydroxyl content, the defect named Non-Bridging Oxygen Hole Center (NBOHC) can occur (Vaccaro 2009). High concentrations of molecular water and hydroxyl are responsible for the formation of greenish color in colorless quartz after exposure to ionizing radiation (Enokihara 2013). Moreover, the high concentration of molecular water indicates rapid crystal growth (Balitsky 1977, Aines and Rossman 1984). Throughout the crystallization of quartz, the water concentration may vary and a decrease in the water content can imply a decrease in the growth rate. This variation can occur even within the same geode, *e.g.*, the development of crystals of intense green along with ones of weaker green, or even colorless or violet crystals (Henn and Schultz-Güttler 2012).

The infrared spectroscopy (IR) technique is used to verify the presence of H_2O and OH, indicating possible color changes after radiation exposure (Müller and Koch-Müller 2009, Nunes *et al.* 2009). According to Lameiras (2012), natural colorless quartz always has the following absorption bands at room temperature: 2,499, 2,600, 2,677, 2,771, 2,935, and 3,063 cm^{-1}. The wavenumber region between 3,200 and 3,600 cm^{-1} is related to color development in colorless quartz under ionizing radiation (Lameiras 2012). The samples with an absorption band at 3,430 (± 10 cm^{-1}) and 3,585 cm^{-1} indicate that the natural colorless quartz could develop violet or grayish-green colors when irradiated (Nunes *et al.* 2009). Exposure to intense ultraviolet radiation, however, can remove the grayish hue (Choong 1945).

The Serra Geral Group has a significant production of amethyst, agate, and colorless quartz, in addition to citrine, which is produced by heating amethyst crystals to around 500 to 600ºC (Fischer 1999). Colorless quartz has a secondary

[1]Programa de Pós-Graduação em Geociências, Instituto de Geociências, Universidade Federal do Rio Grande do Sul – Porto Alegre (RS), Brazil. E-mails: larissatononi@hotmail.com, lauren.duarte@ufrgs.br, mauriciotfm@gmail.com

[2]Laboratório de Gemologia, Instituto de Geociências, Universidade Federal do Rio Grande do Sul – Porto Alegre (RS), Brazil. E-mail: labogem@ufrgs.br

[3]Laboratório de Irradiação Gama, Centro de Desenvolvimento da Tecnologia Nuclear – Belo Horizonte (MG), Brazil. E-mail: fsl@cdtn.br

[4]Laboratório de Pesquisas Gemológicas, Centro da Tecnologia Mineral – Rio de Janeiro (RJ), Brazil. E-mail: jurgen@cetem.gov.br

*Corresponding author.

economic interest, presenting low added-value. However, it can be modified by irradiation, producing a green color variety with better economic value. The green color is just one of the possible results of treatment in colorless quartz by irradiation (Enokihara 2013). This color can also be generated by heating amethyst crystals, mainly from Montezuma (Paradise 1982, Nassau 1983, Rossman 1994, Guttler *et al.* 2011). According to Rossman (1994), the occurrence of naturally green quartz is rare, not quite understood, and still being discussed. Hence, this paper aims to contribute to the understanding of the change of colorless quartz hosted in rhyodacites after gamma irradiation, through infrared study, as well as, to relate the development of color with the water content present in quartz crystals.

GEOLOGICAL SETTING

The Serra Geral Group comprises successive flows of volcanic rocks, mainly of tholeiitic basaltic composition, followed by tholeiitic, andesitic, and rhyodacites-rhyolites. Rhyodacites-rhyolites represent just 3% of the entire volume of the Serra Geral Group (Piccirillo *et al.* 1988). In the regions near Progresso and Nova Bréscia municipalities (Fig. 1), the upper lava flows are composed of acidic volcanic rocks classified as rhyodacites, according to the lithogeochemical classification of De La Roche *et al.* (1980), characterized as Palma type and Caxias do Sul (high-Ti) subgroup (Juchem 2014).

The geode mineralization consists of a huge hydrothermal system by injection of sand and water, including water transportation from underlying Botucatu sandstone (Duarte and Hartmann 2014), which reached volcanic rocks and mineralized the host rock in an epigenetic event (Duarte *et al.* 2009, Hartmann *et al.* 2012). Therefore, water was largely available during the formation of quartz by hydrothermal mineralization.

The mineralization of gemological quartz varieties occurs partially or completely in the geodes. The geode filling is characterized by mineralization of a thin outer layer of chalcedony, which may be banded (agate), followed by a layer of colorless quartz, which may or may not develop a progressive increase to violet color (amethyst variety). The mineralized level of the geodes in the regions of Progresso and Nova Bréscia is described by Juchem (2014) as black colored rocks and resinous appearance (pitchstone), interspersed with gray to brownish-gray rocks with aphanitic to aphyric texture. Figure 2 shows the lava front mine of the Nova Bréscia and Progresso mines. In those regions, the sporadic exploitation of amethyst and colorless quartz contributes to the regional economy. The extracted quartz crystals have gemological potential.

MATERIALS AND METHODS

The selected samples are fragments of natural colorless quartz crystals with a thickness between 0,5 to 2 mm. Seventeen samples from the regions of Nova Bréscia and Progresso (Rio Grande do Sul State, Southern Brazil) were analyzed. The samples from Nova Bréscia, named NB1 and NB3, were respectively mined in rhyodacites at the elevations of 400 and 490 m. The mine located in Progresso also occurs in a rhyodacite flow, at the elevation of 560–570 m (Fig. 3), and is referred to as PRa. Since it was possible to observe a yellowish hue in some samples collected in this mine, they were divided into two groups, the yellowish group being designated PRa-IA, and the colorless group, PRa-II. A second mine in the Progresso region, named PRb, underlies PRa at the elevation of 520 m, and a vitreous rock of rhyodacitic composition hosts its geodes.

Most samples have transparency with great visual optical quality. All samples were sawn without crystallographic orientation or polishing. The samples were investigated before irradiation by infrared spectrometry applying the Fourier-transform (FTIR) technique at the *Laboratório de Pesquisas Gemológicas* (Lapege) in the *Centro de Tecnologia Mineral* (CETEM), using a Perkin Elmer® spectrometer, model Spectrum 400, with 4 cm^{-1} resolution and 16 scans at room temperature, and using the region comprising the near-infrared, 4,000-2,500 cm^{-1}. The spectra were normalized according to wavenumber 2,681 cm^{-1}, corresponding to an absorption value of 1. This wavenumber was selected as the average between 2,674 and 2,691 cm^{-1}, obtained in the samples, and this absorption band is present in all samples and unaffected by irradiation (Nunes *et al.* 2009). A baseline correction method was applied to compare different samples.

To calculate the Amethyst Factor (f_a), the method of Lameiras (2012) was applied. This method previously determines the color obtained after colorless quartz is exposed to gamma irradiation: whether it will be green or violet. Variable f_a is calculated using the following equation (Equation 1):

$$f_a = \frac{h_1}{h_2} \quad (1)$$

in which:

h_1 = the height of the band, 3,441 cm^{-1};

h_2 = the minimum height between 3,441 and 3,585 cm^{-1}.

According to Lameiras (2012), samples with $f_a > 2.7$ may develop violet color after irradiation with a dose greater than 200 kGy (Gy = Gray; absorbed radiation dose unit); if $f_a < 2.7$, the sample can develop grayish-green color with doses greater than 600 kGy; if the f_a is between 2.7 and 3.3, colors between violet and green may develop, but without commercial value. Concomitantly, it is necessary to calculate the area under the spectrum between wavenumbers 3,000 and 3,600 cm^{-1}. This area is associated with water content and trace elements, which control the changing color after gamma radiation exposure, being represented by a broad band in this region (Lameiras 2012). In this case, the influence of the water content is greater since prasiolite in hydrothermal regions typically has higher levels of it, which differs from amethyst, as reported by Guttler (2007), Hebert and Rossman (2008), and Enokihara (2013). Also, according to Lameiras (2012), the calculated area is complementary to f_a. For a $f_a < 2.7$, if the calculated area is < 900 or > 900, the sample will develop a grayish-green color after irradiation at 600 kGy. Otherwise, if the calculated area is <

200 or > 200, the dose to be applied is 200 kGy, and the color obtained will be violet.

The samples of quartz crystals were submitted to gamma irradiation with dry cobalt-60 source and exposed to 900 kGy doses in an MDS Nordion Category II Multi-Purpose Panoramic Irradiator, Model/Serial Number IR-214 and type GB-127 at the *Laboratório de Irradiação Gama* (LIG) in the *Centro de Desenvolvimento da Tecnologia Nuclear* (CDTN). The color change was estimated visually and, subsequently, compared to untreated samples and pre-irradiation photographs.

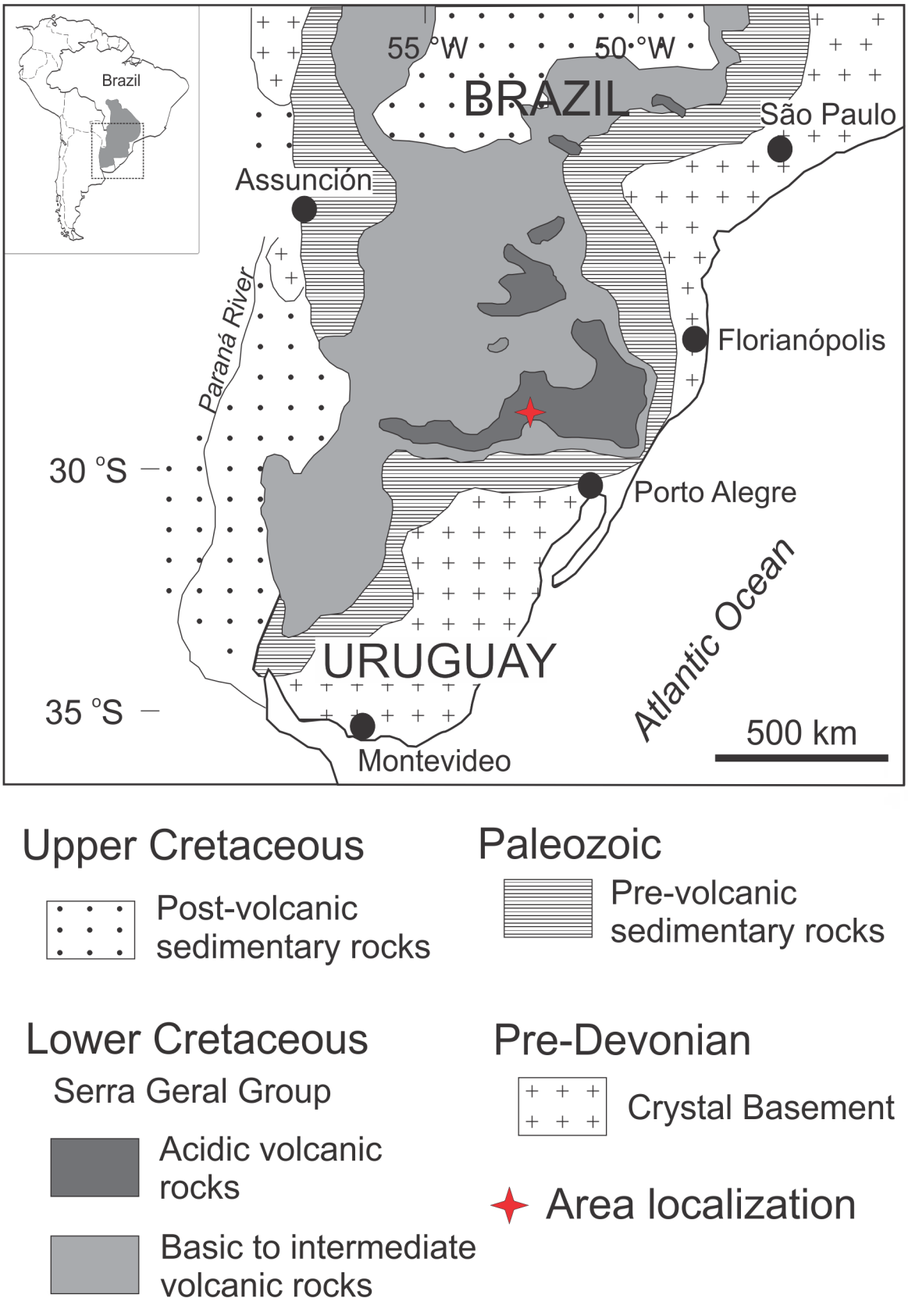

Source: modified from Gilg *et al.* (2003)

Figure 1. Simplified geological map of the Paraná Basaltic Province, with indication of the studied area.

After irradiation, two samples from Progresso (PRa-IA and PRa-II) were submitted to Thermogravimetric analysis (TGA), performed on a TGA Discovery (TA Instruments) at the *Laboratório Multiusuário de Análise Térmica* (LAMAT) of the *Instituto de Química, Universidade Federal do Rio Grande do Sul* (UFRGS). Approximately 30 mg of the powder samples were heated in a platinum high-temperature (HT) crucible from 20 to 1,000ºC, at a heating rate of 10ºC/min, with an initial temperature of 25ºC, and nitrogen gas flow at 25 mL/min. One of the samples has two different colors in its extremities, greenish and colorless, so it was sawn in two halves — colorless and greenish PRa-II — for separate analysis.

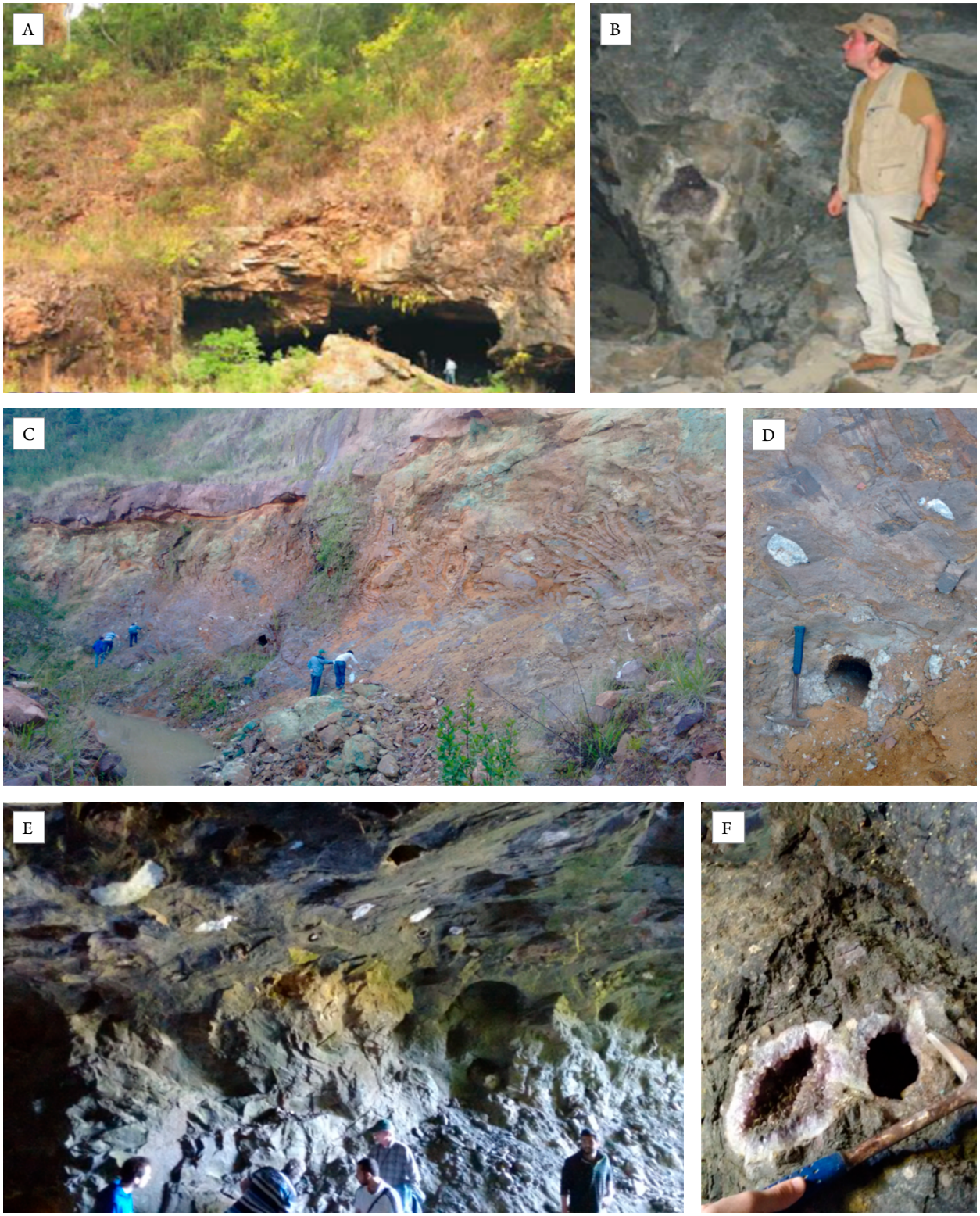

Figure 2. Mining front in the regions of Nova Bréscia and Progresso. (A) Underground gallery at the mineralized level in the region of Nova Bréscia; (B) detail of the amethyst geode on the mineralized level inside the pit of Figure A. Modified from Juchem (2014); (C) mining activity in the region of Progresso (PRa-II and PRa-IA samples); (D) detail of full and partially full geodes from Figure C; (E) interior of the mine from where the PRb samples were taken, observe the completely filled geodes at the top of the gallery; (F) detail of partially filled amethyst geodes, located in the same gallery shown in Figure E.

RESULTS

The analysis was performed considering the region between 3,200 and 3,600 cm^{-1}, which provides information about trace elements. Figure 4 shows the spectra obtained from the samples. They exhibit a spectrum pattern with a sharp band at 3,585 cm^{-1} (± 1 cm^{-1}) and a broad band ranging from 3,428 to 3,445 cm^{-1}. Also, all samples show small bands at 2,681 (± 8 cm^{-1}) and at 2,600 cm^{-1} (± 8 cm^{-1}), which are always present in quartz and do not change after irradiation (Lameiras 2012). The spectra obtained show noises at 3,500 to 4,000 cm^{-1}, normally due to microinclusions or internal turbidity (Hebert and Rossman 2008), and in the 3,500 cm^{-1} range those noises may be related to the unpolished fragment used in the analysis.

All samples from the NB1 group showed a pattern of spectra (Fig. 4A), peaking at 3,585 cm^{-1} and a broad band with values from 3,429 to 3,445 cm^{-1}. Also, it is possible to visualize small bands at ~2,680 and ~2,594 cm^{-1}. Sample NB1-C exhibits the highest absorption intensity when compared to other samples from the same group, while sample NB1-A shows the lowest intensity and a very small shoulder at ~3,198 and ~3,298 cm^{-1}. Samples NB1-B and NB1-C present noise between 3,400 and 3,585 cm^{-1} and show a small band at 3,564 cm^{-1}.

The spectra of NB3 samples (Fig. 4B) exhibits a sharp band at 3,585 cm^{-1} and a broad band varying between at 3,430 and 3,435 cm^{-1}. Also, it is possible to visualize bands at 2,680 (± 5 cm^{-1}) and 2,600 (± 5 cm^{-1}). The highest absorption intensity of this group is shown by NB3-C, while NB3-B exhibits the lowest intensity for the samples of the same group.

The PRa-II and PRa-IA samples show similar absorption spectra patterns (Figs. 4C and 4D), with a sharp band at 3,585 cm^{-1} (± 1 cm^{-1}) and a broad band between 3,428 and 3,445 cm^{-1}, both also show noise between ~3,440 and 3,585 cm^{-1}. The PRa-IA-A sample shows a less prominent band, at 3,585 cm^{-1}. The PRa-II-C sample exhibits, in addition to the absorption band at 3,585 and 3,445 cm^{-1}, two small bands, at ~2923 and ~2853 cm^{-1}. The samples PRa-II and PRa-IA present a small band at 3,564 and 3,566 cm^{-1}, possibly due to sample noise in the analysis. Also, samples of PRa-II and PRa-IA groups have small bands at 2,684 (± 4 cm^{-1}) and 2,602 (± 3 cm^{-1}).

Figure 4E shows the spectra of PRb. The samples in this group show a sharp band at 3,585 cm^{-1} (± 1 cm^{-1}) and a broad band between 3,430 and 3,440 cm^{-1}. Samples PRb-A, PRb-B, and PRb-C present a narrower band in the region around 3,400 cm^{-1} when compared to the other samples analyzed. Additionally, these samples present a shoulder from ~3,472 to ~3,478 cm^{-1}. The samples of PRb-D and PRb-E show different spectra compared to other samples from the same group: the band at 3,585 cm^{-1} is less prominent, there is an enlargement

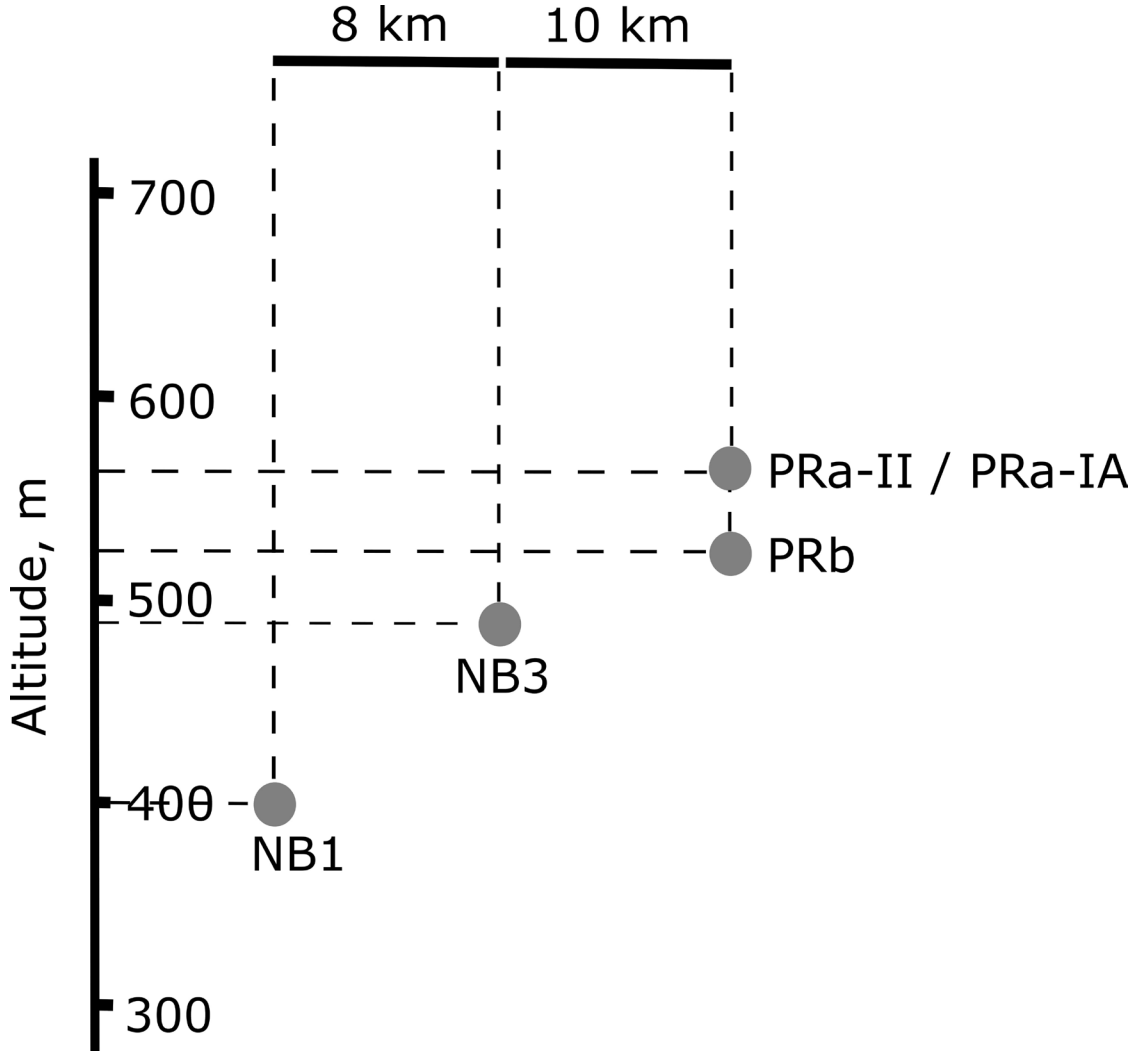

Figure 3. Schematic diagram showing elevation and distance of the studied points.

approximately at 3,200 cm^{-1}, and they show greater noise in the range from 3,400 to 3,585 cm^{-1}. Moreover, all samples from this group exhibit small bands at 2,680 (± 2 cm^{-1}) and 2,603 (± 4 cm^{-1}).

Amethyst Factor (f_a) value and area calculation from the samples are shown in Table 1. All samples present values < 2.7, indicating that they will turn green after irradiation. According to Lameiras (2012), a quartz crystal with f_a value < 2.7 should receive a minimum radiation dose of 600 kGy to develop green color. The samples were submitted to a dose of 900 kGy of gamma irradiation to increase the chances of positive results and to observe their behavior. All samples were

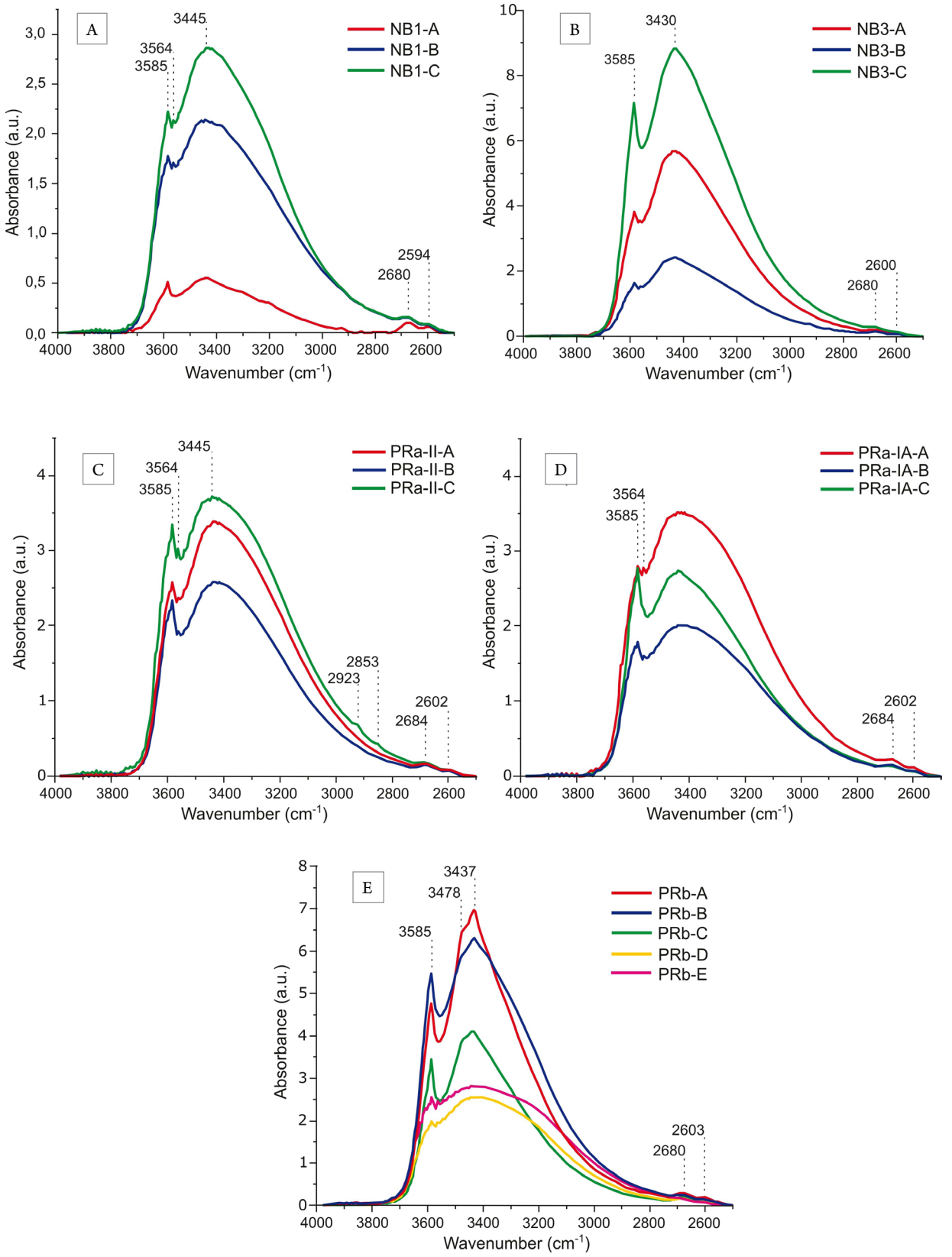

Figure 4. Infrared absorption spectrum of the samples: (A) NB1; (B) NB3; (C) PRa-II; (D) PRa-IA; (E) PRb. The samples have the similar absorption bands.

colorless quartz (Fig. 5), except PRa-IA, which was slightly yellowish (Fig. 5D), and all the analyzed samples changed colors after irradiation, as shown in Figure 6.

Samples from the NB1 group developed two colorations along the crystal (Fig. 6A). The inferior portion of the crystal became green, while the superior portion became a phantom amethyst crystal. It is also possible to visualize a colorless part in the intermediate region of each crystal. Fragments of NB1-A and NB1-C, as well as other samples from the same group, did not present the amethyst phantom crystal, and present slight zoning between colorless and greenish color. Sample NB1-B presents a dark gray band at a portion of the crystal and grayish at another portion.

The NB3 samples obtained a more uniform coloration of grayish-green after irradiation than the other samples of this study (Fig. 6B). A crystal from this group presents a weak color zoning, while at one portion it became grayish-green, at the other, it became gray. Samples NB3-A, NB3-B, and NB3-C show predominantly greenish-gray coloration, while the NB3-C sample obtained gray color and low saturation green.

All samples of the PRa-II group developed color zoning, obtaining colorless/grayish color at a portion of the crystal and greenish-gray at the other (Fig. 6C). The samples are predominantly grayish, while one sample of the group became purplish gray. The PRa-II-A and PRa-II-B samples show color zoning with one colorless/grayish portion and one gray portion. These samples exhibit a small strip of amethyst color on the top of the crystal. The PRa-II-C shows color zoning with a grayish-green and slightly purplish coloration.

The PRa-IA samples were initially a yellowish hue, and, after irradiation, a change to grayish-green coloration (Fig. 6D) occurred. In this group, one crystal presented a slightly more intense gray color, becoming completely gray after irradiation. Samples from this group generally show a more uniform greenish-gray coloration, while continue to have faint gray to grayish-green zoning.

The PRb samples exhibit light green coloration after irradiation (Fig. 6E). Sample PRb-A shows a predominantly uniform green coloration, while sample PRb-B shows zoning between green and very weak gray colors. PRb-C, PRb-D, and PRb-E samples also show zoning between green and slightly grayish.

Figure 7 and Table 2 presents the results of TGA analysis for some of the selected samples. H_2O content is shown in percentage, and in parts per million (ppm) for samples from Progresso mine (PRa-IA and PRa-II).

Sample PRa-IA, during heating, kept a stable weight up to 260°C, when it started to lose mass until reaching 1,000°C, having a total loss of 0.15% weight. Sample

Table 1. Amethyst Factor of studied samples.

Sample	f_a	Area calculation (3,000 a 3,600 cm^{-1})
NB1-A	1.49	209
NB1-B	1.29	952
NB1-C	1.40	1,228
NB3-A	1.63	2,194
NB3-B	1.67	947
NB3-C	1.52	3,399
PRa-II-A	1.48	1,432
PRa-II-B	1.39	1,099
PRa-II-C	1.30	1,632
PRa-IA-A	1.32	1,592
PRa-IA-B	1.31	920
PRa-IA-C	1.29	1,155
PRb-A	1.80	2,326
PRb-B	1.41	2,491
PRb-C	1.67	1,440
PRb-D	1.38	1,158
PRb-E	1.26	1,368

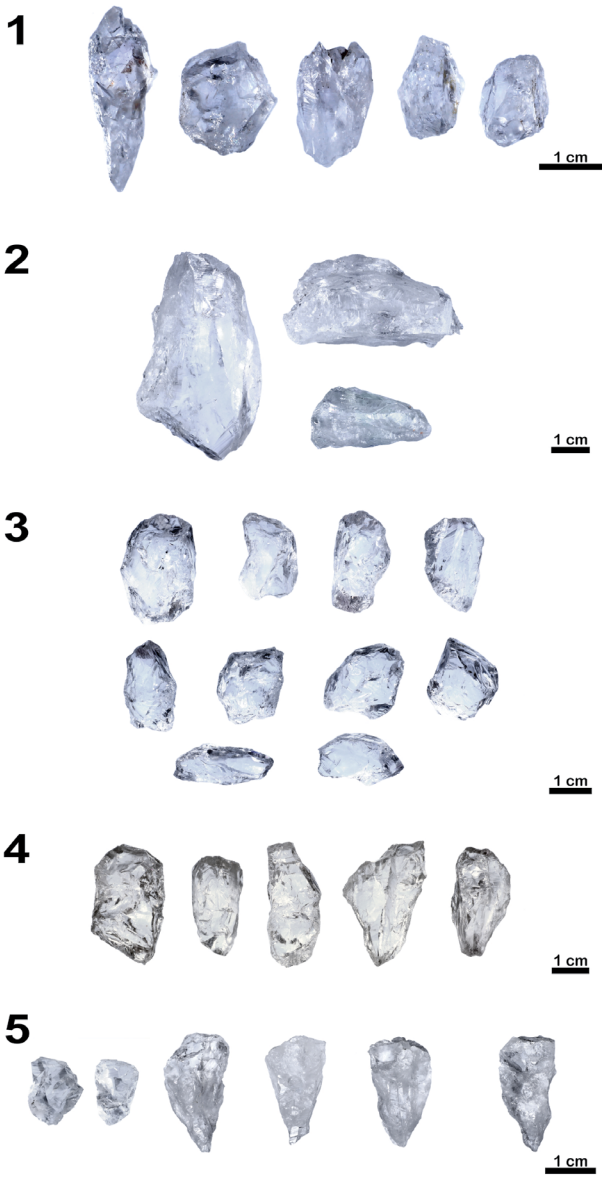

Figure 5. Representative samples of each group studied. It is possible to observe the yellowish hue of the PRa-IA sample. (A) NB1; (B) NB3; (C) PRa-II; (D) PRa-IA; (E) PRb. Photos by Luiz Flavio Lopes.

PRa-II presents zoning, having a colorless/grayish zone and a greenish zone, as shown in Figure 6C; thus, it was tested separately. The colorless/grayish PRa-II sample had a mass loss of 0.50%, remaining stable up to 170ºC and starting to lose mass from 180 to 1,000ºC. While the greenish PRa-II sample remained stable up to 270ºC, starting to lose weight at 280ºC, until it reached 1,000ºC with a mass loss of 0.31%.

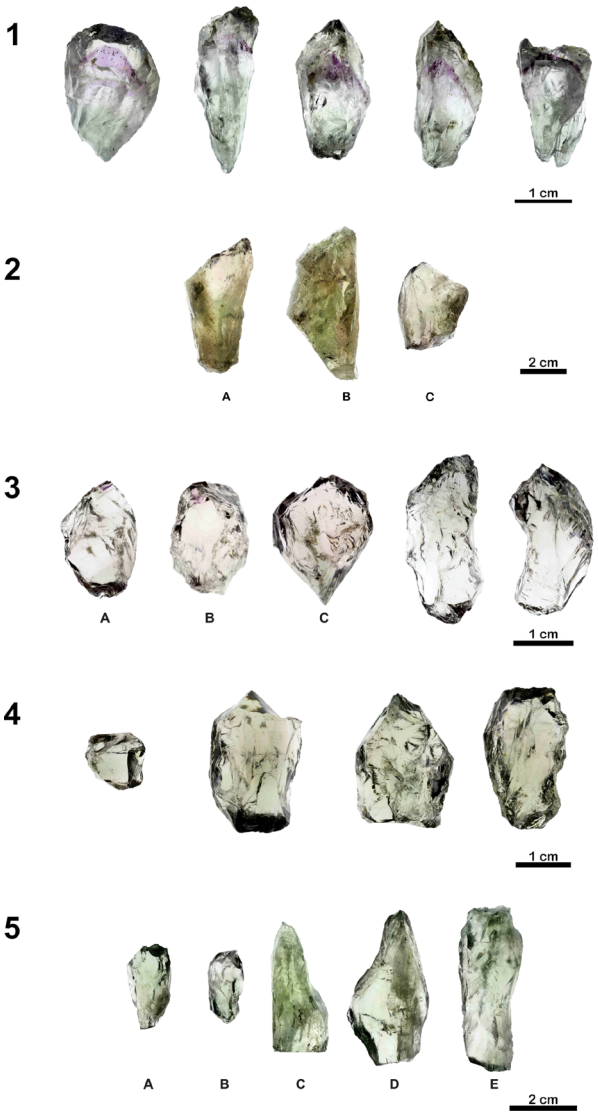

Figure 6. Samples after gamma radiation exposure. (A) Representative samples of the NB1 group, these samples show defined color zoning; (B) samples from the NB3 group. These samples obtained a uniform grayish-green coloration after irradiation. NB3-C sample obtained gray and weak green colors; (C) samples from PRa-II group. PRa-II-A and PRaII-B samples show a small strip of amethyst on the top of the crystal, represented by a dashed line; these samples also show color zoning from colorless/grayish at one end to gray at the other. PRa-II-C shows color zoning from grayish green at one end to slightly purplish at the other; straight lines indicate grayish-green color. The other two samples are representative of the rest of the PRa-II group: the base of the crystal turned colorless/grayish, whereas the top obtained a greenish-gray color; (D) samples representative of the PRa-IA group. These samples generally show a more uniform greenish-gray coloration but still have a faint gray to grayish-green zoning; (5) Samples from PRb group. These samples showed a light green coloration after irradiation and diffuse zoning. Photos by Luiz Flavio Lopes.

DISCUSSION

The results indicate that colorless quartz hosted in geodes in rhyodacites of the Serra Geral Group develops grayish-green color after irradiation. This is based on the results of the IR analysis after exposure to ionizing radiation (gamma rays). Some samples exhibited weak zoning, while others developed the purple gemological variety, amethyst.

The quartz crystals which developed grayish-green or violet color after exposure to gamma irradiation present absorption at 3,585 cm^{-1} wavenumber and at a wide-band at 3,430–3,440 cm^{-1}, as also presented by Lameiras (2012). This absorption behavior was observed in all the samples analyzed. For absorption at 3,585 cm^{-1}, Nunes *et al.* (2009) suggest that it is probably due to the presence of iron, since it occurs in quartz samples which could develop green (prasiolite variety) and violet (amethyst variety) colors after irradiation. Absorption at the 3,400 cm^{-1} wavenumber region is related to Si-OH bonds (Aines and Rossman 1984), which, in turn, are related to the water content. The potential for color development is directly related to the absorption area in the spectra: larger areas in the spectrum are associated with greater potential for color development (Lameiras 2012). According to Guttler *et al.* (2009), the high water content is responsible for the formation of Si-OH bonds, which generates green color in hydrothermal quartz.

Bands ranging from 2,499 to 2,771 cm^{-1} are always present in quartz, and were identifiable in all the samples analyzed. These bands are unaffected by irradiation and unrelated to the color center formation by exposure to gamma radiation. The bands at 3,202 and 3,303 cm^{-1} (± 10 cm^{-1}) are related to overtone or combinations of the Si-O lattice and are always present. According to Lameiras (2012), these bands are not associated with color development after irradiation and they are visible in sample NB1-A. However, this sample presents weak zoning after irradiation, from colorless to weak green, and shows a lower absorption area in the IR spectrum when compared to other samples (see Fig. 4A). This contradiction may occur because the region of the sample measured by the IR spectrum before irradiation remained colorless after the process.

Widening of the band at approximately 3,200 cm^{-1} in samples PRb-D and PRb-E may be caused by OH^-, as cited by Kats (1962), or by different rates of OH/H_2O incorporation trough different growth sectors. Fluid inclusions, which are normally aqueous and monophasic for hydrothermal quartz in this kind of deposit (Gilg *et al.* 2003, Duarte *et al.* 2011), indicate water availability for Si-OH bond.

The samples analyzed generally have similar wavenumbers and f_a values favorable to the development of green color, although with a predominance of grayish-green and greenish-gray colors. There are yet no studies addressing the gray color of these samples, but a relation to aluminum can be hypothesized since this element has been identified in the host rocks (Juchem 2014), as well as in other occurrences of hydrothermal quartz (Hebert and Rossman 2008).

All samples present absorbance area values greater than 900 (Tab. 1), except for NB1-A, which presents a value of 209. Lameiras (2012) establishes that quartz crystals with absorbance area values < 900 will develop grayish-green color after

irradiation, which can be modified either to weak gray after exposure to ultraviolet radiation, to colorless or even weak yellow after irradiation with subsequent heating treatment. With values > 900, colorless quartz becomes grayish green after irradiation, green after exposure to ultraviolet radiation, and colorless or yellow after irradiation with subsequent heating treatment. In this way, the NB1-A sample may not develop green hue (without the tone of gray) if exposed to ultraviolet radiation. After gamma irradiation, some samples presented different behaviors, mainly some crystals from the Nova Bréscia area (NB1 group). Crystals in this group presented conspicuous zoning, generating an amethyst "phantom crystal". This corroborates the relation of the potential development of amethyst color with ionizing radiation (Berthelot 1906 *apud* Rossman 1994, Lehmann and Moore 1966, Lehmann 1975).

As observed in the results, crystals of greater size allow the visualization of the chemical variation of the fluid through the development of color zoning after irradiation. This can be observed in the samples from the NB1 group, due to the preservation of the apical faces of the crystals. The base of these crystals displays the green color, which had greater availability of water in their fluid at the beginning of crystallization, in the intermediate region stay colorless and in the apical portion violet (see Fig. 6A). This corroborates with Hebert and Rossman (2008), Guzzo *et al.* (2009), and Enokihara (2013) with a higher concentration of OH and H_2O in the initial crystallization phase and that water concentration decreases throughout the development of the crystal, allowing the formation of purple color related to center color based in Fe^{3+}, since the presence of water may inhibit the development of the amethyst (Hebert and Rossman 2008). Moreover, the combination of high doses of radiation might also inhibit the development of Al- and Fe-based color centers (Hashimoto *et al.* 2001, Henn and Schultz-Güttler 2012).

According to Enokihara (2013), molecular water and hydroxyl groups are essential for the development of green color after irradiation in hydrothermal quartz, as they are the agents responsible for the NBOHC defect, with a directly proportional relation between the water content and the intensity of the color obtained. However, in the TGA analysis of Progresso samples, the sample which had the highest loss of water content was the slightly grayish/colorless portion of crystal PRa-II (5,000 ppm), even when compared to the greenish-gray portion of the same crystal (3,100 ppm); it was even higher than the grayish-green sample PRa-IA (1,500 ppm). This may suggest that an excess content of water molecules and hydroxyl groups may inhibit the development of green color. This may justify the colorless region of group samples PRa-II.

The variation in fluid chemistry can sometimes be observed by the color zoning of certain minerals. For samples from some

Table 2. Content of H_2O in percentage and ppm.

Sample	% H_2O	Concentration H_2O (ppm)
PRa-IA	0.15	1,500
PRa-II colorless/grayish	0.50	5,000
PRa-II greenish	0.31	3,100

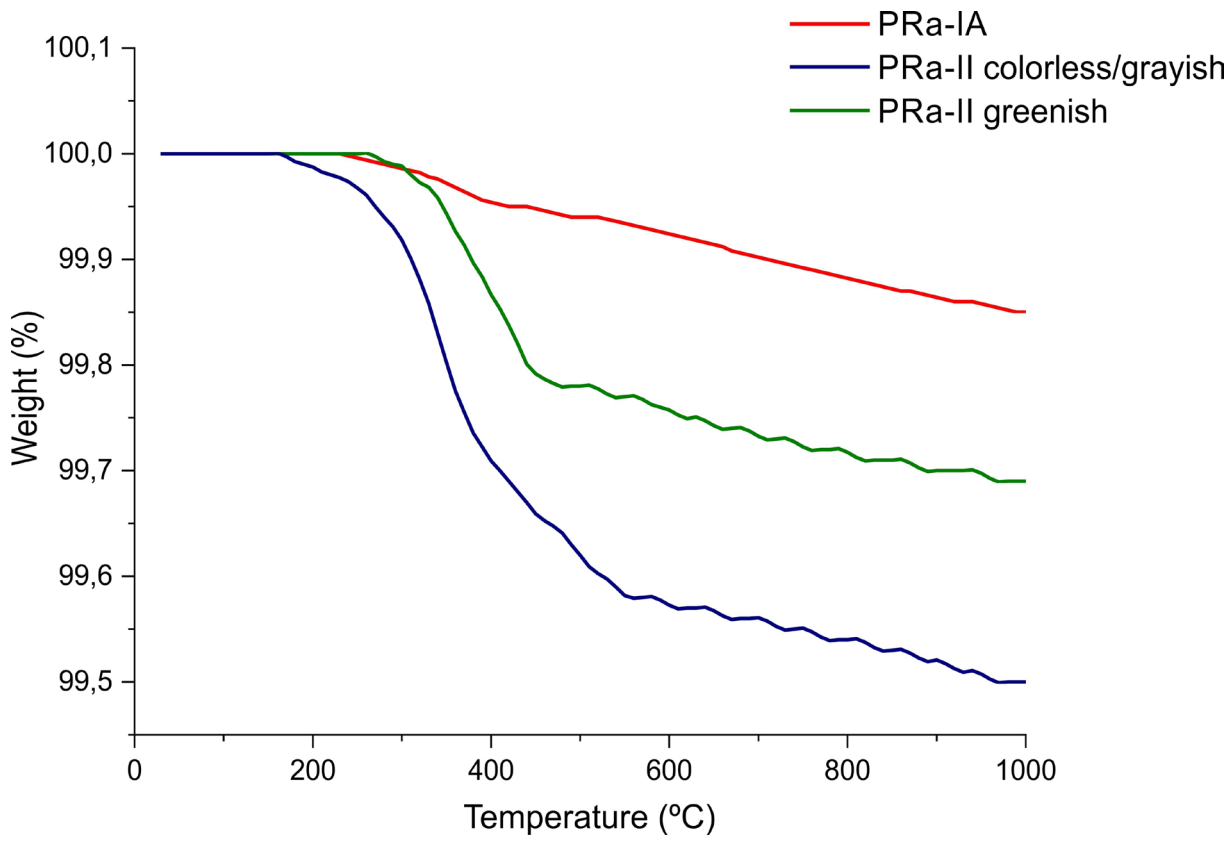

Figure 7. Thermogravimetric analysis from PRa-IA and PRa-II (colorless/grayish and greenish samples) groups. The PRa-II colorless/grayish sample exhibits the greatest loss of mass in H_2O content compared to the other samples.

groups, it is possible to observe the color zoning in the same crystal, which may indicate chemical variation, but, as they have unknown crystallographic orientation, it is not possible to state that these samples had a higher initial concentration of water content compared to the final stage of crystallization.

Color zoning was observed in all samples, with some samples presenting a defined zoning and different colors, and others presenting weak zoning. Furthermore, in all samples, the same crystal exhibits color variation and this may indicate that the water content in the mineralized fluid varied throughout the crystal growth. As most samples have an unknown crystallographic orientation (except NB1 group), it is not possible to state that these samples had a higher initial concentration of water content compared to the final stage of crystallization.

Geode-type mineralization in basalts (Duarte *et al*. 2009, Hartmann *et al*. 2012) is established by a sequence of hydrothermal pulses, which can occasionally be observed in geode fillings by their filling sequence (Duarte *et al*. 2011). The most common sequence in geode fillings consists of chalcedony, fine-grained quartz, and coarse-grained quartz (Duarte *et al*. 2009), with possible repetition of the sequence. Reaction kinetics and availability of elements in the mineralizing fluid change as the systems evolve into a closed system, so that the fluid becomes enriched in water and other elements (Wang and Merino 1990). However, as observed for this kind of deposit (Duarte *et al*. 2009), the system can be considered open, and these relations might be superimposed, as the fluid might receive increments of water and other elements with each new mineralizing pulse, interfering with the crystal color and their chemistry and impurities. This shows that even quartz in geodes from extremely close regions may differ in chemical influences due to their open system.

It should also be taken into account that, according to Nassau (1984), the use of gamma-ray radiation produces good color uniformity, which was not the case in the samples of this study. This leads us to suppose that the chemical variation and water availability during crystallization processes influenced the generation of the green color.

CONCLUSIONS

The present study demonstrates the potential for colorless quartz crystals originated from geodes hosted in rhyodacites of the Serra Geral Group to develop the grayish-green color. The analysis in the IR region performed before irradiation indicates potential color changes. Moreover, the Amethyst Factor method was successfully applied, indicating values < 2.7, and all samples changed color after receiving recommended doses of radiation. After exposure to radiation, the crystals have developed:

- from colorless to grayish-green;
- from grayish-green to slightly purplish.

One group of samples developed a color zoning ranging from greenish, through colorless, to an amethyst phantom crystal in its apical portion. This may suggest variation in the water content throughout crystallization, which was also observed by thermogravimetric analysis, indicating a subtle variation of the elements which enable the creation of NBOHC color centers. Even with a possible directly proportional relation between the water content and the intensity of the color obtained, the results suggest that an excessive concentration of H_2O might inhibit the development of grayish-green color under radiation exposure. However, meticulous studies regarding the varying water content along the crystal prism, the presence of trace elements, and the origin of grayish color are necessary. Also, to establish the relation of these factors to the development of color zoning is required to obtain more detailed data. In addition to further study on NB1 samples for possible gemological purposes.

ACKNOWLEDGMENTS

This work was financially supported by the Conselho Nacional de Desenvolvimento Científico e Tecnológico (CNPq) Project 454183/2014-3. The authors thank Flávio Antônio Zanchettin for the samples of Progresso, Luiz Flavio Pereira Lopes for the photographs, Danielle Gomides Alkmim for the technical support, Pedro Luis Ammon Xavier for the review, and Leo Afraneo Hartmann for the support to publish this paper.

ARTICLE INFORMATION

Manuscript ID: 20190114. Received on: 10/22/2019. Approved on: 05/21/2020.

L.L.T. wrote the first and last draft of the manuscript and prepared Figures 1 to 7. L.C.D. was an advisor during the writing of the manuscript, provided advisorship regarding Serra Geral Group, improved the manuscript through corrections and suggestions. P.L.J. provided part of the analyzed samples and improved the manuscript through corrections and suggestions. F.S.L. provided preparation and irradiation of samples of the manuscript. J.S. assisted in FTIR analysis of the samples and improved the manuscript. M.T.F.M. assisted in the preparation and treatment of the data.

Competing Interests: The authors declare no competing interests.

REFERENCES

Aines R.D., Rossman G.R. 1984. Water in minerals? A peak in the infrared. *Journal of Geophysical Research*, **89**(B6):4059-4071. https://doi.org/10.1029/JB089iB06p04059

Balitsky V.S. 1977. Growth of large amethyst crystals from hydrothermal fluoride solutions. *Journal of Crystal Growth*, **41**(1):100-102. https://doi.org/10.1016/0022-0248(77)90102-6

Choong S.P. 1945. Coloration and luminescence produced by radium rays in the different varieties of quartz, and some optic properties of these varieties. *Proceedings of the Physical Society*, **57**(1):49-55.

De La Roche H., Leterrier J., Grandclaude P., Marchal M. 1980. A classification of volcanic and plutonic rocks using R1R2 – diagram and major-element analyses – ITS relationships with current nomenclature. *Chemical Geology*, **29**(1-4):183-210. https://doi.org/10.1016/0009-2541(80)90020-0

Duarte L.C., Hartmann L.A., Ronchi L.H., Berner Z., Theye T., Massonne H.J. 2011. Stable isotope and mineralogical investigation of the genesis of amethyst geodes in the Los Catalanes gemological district, Uruguay, Southernmost Paraná Volcanic Province. *Mineralium Deposita*, **46**:239-255. https://doi.org/10.1007/s00126-010-0323-6

Duarte L.C, Hartmann L.A., Vasconcellos M.A.Z., Medeiros J.T.N., Theye T. 2009. Epigenetic formation of amethyst-bearing geodes from Los Catalanes gemological district, Artigas, Uruguay, southern Paraná Magmatic Province. *Journal of Volcanology and Geothermal Research*, **184**(3-4):427-436. https://doi.org/10.1016/j.jvolgeores.2009.05.019

Duarte S.K., Hartmann L.A. 2014. Evolução dos injetitos de areia do Complexo Novo Hamburgo, Província Vulcânica Paraná. *In*: Hartmann L.A, Baggio S.B. (Eds.). *Metalogenia e Exploração Mineral no Grupo Serra Geral*. Porto Alegre: IGEO/UFRGS. p. 203-232.

Enokihara C.T. 2013. *Estudo do quartzo verde de origem hidrotermal tratado com radiação gama*. PhD Thesis, Universidade de São Paulo, São Paulo, 165 p.

Fischer A.C. 1999. *Composição química e possíveis causas de cor da ametista da região do Alto Uruguai, RS*. MS Dissertation, Universidade Federal de Ouro Preto, Ouro Preto, 168 p.

Gilg H.A., Morteani G., Kostitsyn Y., Preinfalk C., Gatter I., Strieder A.J. 2003. Genesis of amethyst geodes in basaltic rocks of the Serra Geral Formation (Ametista do Sul, Rio Grande do Sul, Brazil): a fluid inclusion, REE, oxygen, carbon, and Sr isotope study on basalt, quartz, and calcite. *Mineralium Deposita*, **38**(8):1009-1025. 10.1007/s00126-002-0310-7

Guttler R.A.S. 2007. Quartzo verde ou prasiolita? *Diamond News*, **28**:19.

Guttler R.A.S., Enokihara C.T., Helfenberger A.F.M., Rela P.R. 2011. Montezuma prasiolite: Gamma radiation effects. *In*: International Nuclear Atlantic Conference; Meeting on Nuclear Applications, 10.; Meeting on Reactor Physics and Thermal Hydraulics, 17.; Meething on Nuclear Industry, 2., 2011. *Annals*... Belo Horizonte.

Guttler R.A.S., Enokihara C.T., Rela P.R. 2009. Characterization of color centers in quartz induced by gamma irradiation. *In*: International Nuclear Atlantic Conference, 9., 2009. *Annals*... Rio de Janeiro.

Guzzo P.L., Miranda M.R., Luz A.B. da. 2009. Espectroscopia infravermelha à baixa temperatura em quartzo e ametistas com altas concentrações de OH e H_2O. *Revista Escola de Minas*, **62**(3):349-356. https://doi.org/10.1590/S0370-44672009000300013

Hartmann L.A., Duarte L.C., Massonne H.J., Michelin C., Rosenstengel L.M., Bergmann M., Theye T., Pertille J., Arena K.R., Duarte S.K., Pinto V.M., Barboza E.G., Rosa M.L.C.C., Wildner W. 2012. Sequential opening and filling of cavities forming vesicles, amygdales and giant amethyst geodes in lavas from the southern Paraná volcanic province, Brazil and Uruguay. *International Geology Review*, **54**(1):1-14. https://doi.org/10.1080/00206814.2010.496253

Hashimoto T., Fujita H., Hase H. 2001. Effects of atomic hydrogen and annealing temperatures on some radiation-induced phenomena in differently originated quartz. *Radiation Measurements*, **33**(4):431-437. https://doi.org/10.1016/S1350-4487(00)00140-2

Hebert L.B., Rossman G. 2008. Greenish quartz from Thunder Bay Amethist Mine Panorama, Thunder Bay, Ontario, Canada. *The Canadian Mineralogist*, **46**(1):111-124. http://dx.doi.org/10.3749/canmin.46.1.111

Henn U., Schultz-Güttler R. 2012. Review of some current coloured quartz varieties. *The Journal of Gemmology*, **33**(1-4):29-43.

Juchem P.L. 2014. Amethyst mineralization in rhyodacites of the Serra Geral Group, Paraná volcanic province. *In*: Hartmann L.A., Baggio S.B. (Eds.). *Metallogeny and mineral exploration in the Serra Geral Group*. Porto Alegre: IGEO/UFRGS. p. 321-334.

Kats A. 1962. Hydrogen in alpha-quartz. *Philips Research Reports*, **17**:133-195.

Lameiras F.S. 2012. The relation of FTIR signature of natural colorless quartz to color development after irradiation and heating. *In*: Morozhenko V. (Ed.). *Infrared Irradiation*. London: InTechOpen. p. 41-56. http://doi.org/10.5772/35738

Lehmann G. 1975. On the color centers of iron in amethyst and synthetic quartz: A discussion. *American Mineralogist*, **60**(3-4):335-337.

Lehmann G., Moore W.J. 1966. Optical and paramagnetic properties of iron centers in quartz. *The Journal of Chemical Physics*, **44**:1741-1745. https://doi.org/10.1063/1.1726932

Müller A., Koch-Müller M. 2009. Hydrogen speciation and trace element contents of igneous, hydrothermal and metamorphic quartz from Norway. *Mineralogical Magazine*, **73**(4):569-583. https://doi.org/10.1180/minmag.2009.073.4.569

Nassau K. 1983. *The physics and chemistry of color:* the fifteen causes of color. New York: John Wiley & Sons. 454 p.

Nassau K. 1984. *Gemstone Enhancement*. Los Angeles, Butterworths, 221 p.

Nunes E.H.M., Melo V., Lameiras F., Liz O., Pinheiro A., Machado G., Vasconcelos W. 2009. Determination of the potential for extrinsic color development in natural colorless quartz. *American Mineralogist*, **94**(7):935-941. https://doi.org/10.2138/am.2009.3043

Paradise T.R. 1982. The natural formation and occurrence of green quartz. *Gems and Gemology*, **18**(1):39-42. https://doi.org/10.5741/GEMS.18.1.39

Piccirillo E.M., Comin-Chiaramonti P., Bellieni G., Civetta L., Marques L. S., Melfi A.J., Petrini M.I.B., Raposo M.I.B., Stolfa D. 1988. Petrogenetic aspects of continental flood basalt-rhyolite suites from the Paraná Basin (Brazil). *In*: Piccirillo E.M., Melfi A.J. (Eds.). *The Mesozoic Flood Volcanism of the Paraná Basin - petrogenetic and geophysical aspects*. São Paulo: USP/Inst. Astronômico e Geofísico. p. 179-205.

Rossman G.R. 1994. Colored varieties of the silica minerals. *Reviews in Mineralogy*, **29**:433-467.

Salh R. 2011. Defect related luminescence in silicon dioxide network: a review. *In*: Basu S. (Ed.). *Crystalline Silicon:* Properties and Uses. London: InTechOpen, p. 135-172.

Vaccaro L. 2009. *Electronic and vibrational properties of the Non Bridging Oxygen Hole Center in the bulk and at the surface of silica.* PhD Thesis, Dipartimento di Scienze Fisiche ed Astronomiche, Università degli Studi di Palermo, Palermo, 139 p.

Wang Y., Merino E. 1990. Self-organizational origin of agates: banding, fiber twisting, composition, and dynamic crystallization model. *Geochimica et Cosmochimica Acta*, **54**(6):1627-1638. https://doi.org/10.1016/0016-7037(90)90396-3